TES ATMOSPHERIC TEMPERATURE, AEROSOL OPTICAL DEPTH, AND WATER VAPOR OBSERVATIONS 1999-2004.

M. D. Smith, *NASA Goddard Space Flight Center, Greenbelt, MD, USA (Michael.D.Smith@nasa.gov)*

Introduction:

The Mars Global Surveyor (MGS) began mapping operations from Mars orbit on 1 March 1999 (Mars Year 24, Ls=104°), and provided nearly continuous monitoring of conditions in the Martian atmosphere until 31 August 2004 (Mars Year 27, Ls=81°), or almost three full Martian years. Infrared spectra taken by the Thermal Emission Spectrometer (TES) on-board MGS are very well suited for monitoring Martian atmospheric conditions. The atmospheric thermal structure, dust and water ice aerosol optical depth, and water vapor column abundance can all be retrieved from each TES spectrum, This allows the latitudinal, longitudinal, and seasonal dependences of these quantities to be examined in unprecedented detail. TES builds on earlier spacecraft observations of Mars by Mariner 9 and the Viking orbiters by providing increased spatial and temporal resolution and more complete spatial and seasonal coverage. Comparison of Mariner 9, Viking, and TES results allows interannual variability to be evaluated. Results relating to the retrieval of Mars atmospheric parameters from TES have been made in a number of papers [e.g. first results: *Christensen et al.* 1998; temperature retrieval algorithm: *Conrath et al.,* 2000; Dust optical depth retrieval algorithm: *Smith et al.,* 2000a, b, *Smith* 2004; comparison with ground-based observations: *Clancy et al.,* 2000; water-ice cloud retrieval algorithm: *Pearl et al.,* 2001; derivation of spectral shapes of aerosols: *Bandfield et al.,* 2000; overview: *Smith et al.,* 2001, global dust storm: *Smith et al.* 2002; water vapor retrieval algorithm: *Smith* 2002; interannual variability: *Smith* 2004; aerosol properties: *Wolff and Clancy 2003, Clancy et al. 2003*.].

TES Data Characteristics:

The Thermal Emission Spectrometer (TES) is a thermal infrared interferometer/spectrometer with additional broadband visible and thermal channels (bolometers) [*Christensen et al.,* 1992; 2001]. Six detectors in a three-by-two array simultaneously take spectra covering the spectral range from 200 to 1600 cm^{-1} (6-50 μm), with a selectable spectral resolution of either 6.25 or 12.5 cm^{-1}. A pointing mirror allows TES to observe from nadir to above both the forward and aft limbs, where the atmosphere is observed without direct contribution from the surface. Each pixel subtends a 8.3-mrad field of view.

MGS is in a near-polar, sun-synchronous orbit with the ascending node at 1400 hours. TES data have a spatial resolution of 3 km across-track and 10–20 km along track (because of smear caused by spacecraft motion). The MGS mapping orbit gives one narrow strip of observations running roughly north-south. One day of data gives two sets of twelve such strips spaced roughly 29° apart in longitude, with one set taken near a local time of 0200 hours and the other near 1400 hours. We do not use nighttime data to retrieve aerosol optical depth because 1) the nighttime spectra have lower signal-to-noise, 2) the atmospheric temperature profiles retrieved from nighttime TES data potentially have relatively large uncertainties near the surface due to the near-surface nighttime inversion in the boundary layer, and 3) the large mixture of surface temperature observed over a TES pixel caused by the differences in thermal inertia at scales smaller than a TES pixel.

The primary mode of TES data acquisition is nadir viewing. However, every 10°–20° of latitude around the orbit, a sequence of limb-geometry observations is taken with the field-of-view pointed to observe the atmosphere above the limb. Because the nadir-geometry observations are far more numerous, they are generally used for mapping the spatial distribution of aerosol optical depth. Retrieval of the atmospheric thermal structure uses a combination of observations from nadir-geometry spectra giving information about the lowest 30 km above the surface and limb-geometry spectra giving information from roughly 30-65 km.

Retrieval Methods:

A detailed description of the retrieval algorithms for atmospheric temperatures and aerosol optical depth is given by [*Smith* 2004] (dust), [*Pearl et al.,* 2001] (water-ice), [*Conrath et al.,* 2000] (temperatures), and [*Smith* 2002] (water vapor). Here we describe the retrievals in outline. The retrievals of atmospheric temperature, aerosol optical depth, and water vapor column abundance are performed sequentially. Atmospheric temperatures are retrieved using a constrained linear inversion of radiance in the 15-μm CO_2 band. In this retrieval we account for aerosol optical depth to first order by using an effective surface temperature calculated by taking the brightness temperatures in narrow spectral intervals on either side of the CO_2 band and averaging them. The spectral intervals used are 508-529 and 814-825 cm^{-1}. Temperatures from the surface to ~0.1 mbar (35 km) are obtained from nadir-geometry spectra with a typical vertical resolution of about one scale height (10 km). Temperature profiles can be extracted from 1.0 to 0.01 mbar (65 km), where limb-ge-

ometry spectra are available (typically every 10° in latitude). Complete temperature profiles to 0.01 mbar are obtained by splicing the two temperature profiles through averaging in the 0.1- to 1.0-mbar range. Individual temperature profiles have a typical uncertainty of ~2 K except in the lowest scale height above the ground, where the uncertainty is somewhat larger.

Aerosol optical depth is retrieved after the temperature retrieval is performed. Surface temperature is retrieved along with aerosol optical depth. The basic idea is to find the values of surface temperature and dust and water ice optical depth that provide the best match between computed and observed radiance. Surface emissivity is read from a table (as a function of latitude and longitude), and the strength of minor CO_2 bands is assumed to be a known constant value. The spectral dependence of dust and water ice absorption are taken from the analysis of TES emission phase function (EPF) sequences [*Bandfield and Smith* 2003] and comparisons of spectra taken in nadir and limb geometries. Water vapor is treated in a separate step after the aerosol retrieval, matching the computed strength of five water vapor bands at 240-360 cm^{-1} with the observed spectrum. For both aerosol and water vapor, the retrieval is restricted to those spectra with a surface temperature >220 K. This constraint ensures that there is sufficient thermal contrast between the surface and the atmosphere for an accurate retrieval.

The retrievals use two simplifying assumptions. We assume that (1) the dust is well-mixed with the CO_2 gas and that (2) the aerosols are non-scattering. Water ice and water vapor are not assumed to be well-mixed. The water vapor condensation level is computed using the retrieved temperature profile. Water vapor is confined to below the condensation level, while water ice aerosol is confined to above the condensation level. The assumption of a well-mixed dust has been found to be good in Viking [*Pollack et al.*, 1977; *Jaquin et al.*, 1986], Pathfinder [*Smith et al.*, 1997], and TES data [*Smith et al.*, 2000a]. Therefore, we believe that the error introduced through the well-mixed assumption for dust is small compared to other sources of error and uncertainty in the retrieval.

The second assumption, that the aerosols are non-scattering, has been shown numerically to systematically underestimate the full extinction optical depth (including scattering) by about 30% for dust and by about 50% for water ice [*Smith* 2004; *Wolff and Clancy*, 2003].

Estimated uncertainties in the retrieved values are 2K for temperatures [*Conrath et al.*, 2000], 0.05 or 10% (whichever is larger) for a single aerosol optical depth [*Smith* 2004], and 3 pr-μm or 10% (whichever is larger) for water vapor column abundance [*Smith* 2002]. The above estimate does not include the 30–50% systematic difference between absorption (non-scattering) and extinction (including scattering) optical depth mentioned above.

Overview of TES Atmospheric Observations:

The results presented here were derived using data covering nearly three full Martian yeas from Mars Year 24, Ls=104° (1 March 1999) to Mars Year 27, Ls=81° (31 Aug. 2004). This is the complete set of TES spectrometer observations taken during MGS mapping. In Figure 1 we show dust optical depth (1075 cm^{-1}), the atmospheric temperature at 0.5 mbar, water-ice optical depth (825 cm^{-1}), and water vapor column abundance. Zonal means of daytime (1400 hours) nadir-viewing data are presented. The retrieval of aerosol optical depth and water vapor abundance is restricted to those spectra with a surface temperature >220 K to ensure adequate thermal contrast between the surface and the atmosphere. Because dust optical depth is usually nearly well-mixed with CO_2, it has been scaled to a 6.1-mbar equivalent pressure surface. Water-ice optical depth and water vapor abundance are not as closely well-mixed as dust and so are not scaled.

The current Martian climate has a distinct and generally repeatable dependence on season, latitude, and longitude. In particular, the perihelion season (Ls=180°–360°) is relatively warm, dusty, and free of water ice clouds, while the aphelion season (Ls=0°–180°) is relatively cool, cloudy, and free of dust. Water vapor abundance is largest in both hemispheres near the summer pole. The perihelion season shows a high degree of interannual variability in atmospheric temperature and dust optical depth, primarily associated with the intermittent nature of large dust storms. The aphelion season shows little interannual variability in temperatures and aerosol optical depth. In particular, the low-latitude aphelion-season water ice cloud belt shows a striking repeatability. Water vapor shows moderate interannual variability at all seasons. The largest year-to-year differences are in the southern summer.

Summary:

With nearly three Martian years of regular mapping observations, the MGS TES instrument has provided a rich dataset that can be used to study the seasonal, spatial, and interannual dependence of atmospheric temperature as a function of height, dust aerosol optical depth, water ice cloud optical depth, and water vapor column abundance. Although the TES spectrometer is no longer operational, observations using the visible-wavelength (0.3–3.0 μm) and infrared-wavelength (5–150 μm) bolometers continue. Used in the limb-viewing geometry, bolometer observations can continue to retrieve dust aerosol

optical depth.

References:

Bandfield et al., 2000; *J. Geophys. Res*. **105**, 9573.
Bandfield and Smith 2003. *Icarus* **167**, 47.
Christensen et al., 1992, *J. Geophys. Res*. **97**, 7719.
Christensen et al., 1998, *Science* **279**, 1692.
Christensen et al., 2001, *JGR.* **106**, 22823.
Clancy et al., 2000, *J. Geophys. Res*. **105**, 9553.
Clancy et al. 2003, *J. Geophys. Res.* **108**, doi: 10.1029/2003JE002058.
Conrath et al., 2000, *J. Geophys. Res*. **105**, 9509.
Jaquin et al., 1986, *Icarus* **68**, 442.
Pearl et al., 2001, *J. Geophys. Res*. **106**, 12,325.
Pollack et al., 1977, *J. Geophys. Res.* **82**, 4479.
Smith et al., 1997, *Science* **278**, 1758.
Smith et al., 2000a, *J. Geophys. Res*. **105**, 9539.
Smith et al., 2000b, *J. Geophys. Res*. **105**, 9589.
Smith et al., 2001, *J. Geophys. Res*. **106**, 23,929.
Smith et al., 2002, *Icarus* **157**, 259.
Smith 2002, *JGR.* **107**, doi:10.1029/2001JE001522.
Smith 2004, *Icarus* **167**, 148.
Wolff and Clancy 2003. *J.Geophys. Res.* **108**, doi:10.1029/2003JE002057.

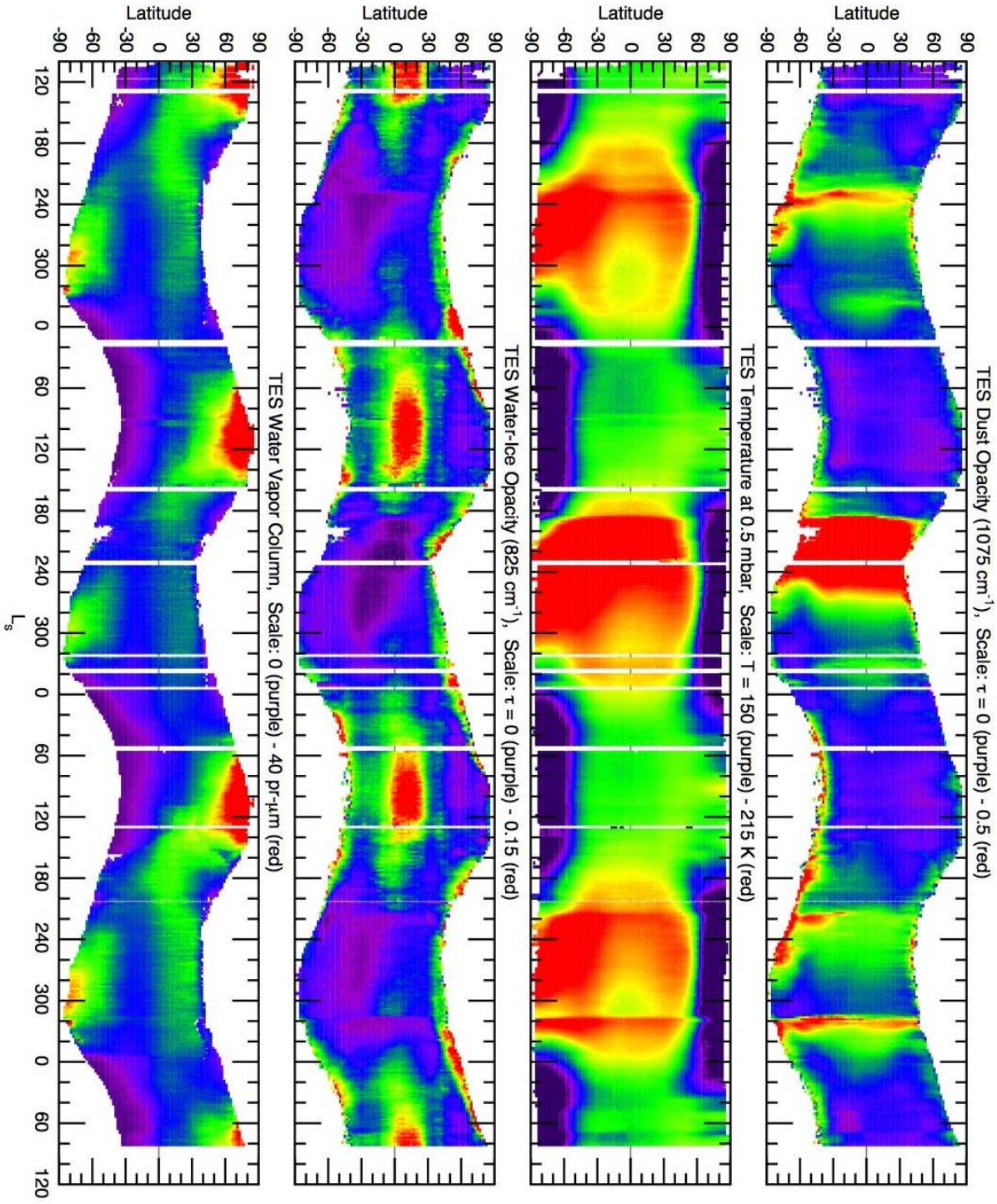

Figure 1. An overview of TES daytime (local time ~ 1400 hours) atmospheric retrievals. Shown is the zonal average of each quantity as a function of latitude and season (Ls) between Mars Year 24, Ls=104° (1 March 1999) and Mars Year 27, Ls=81° (31 August 2004). (Top) Dust optical depth at 1075 cm^{-1} scaled to an equivalent 6.1 mbar pressure surface to remove the effect of topography. (2nd) Atmospheric temperature at 0.5 mbar (~25 km above a nominal 6.1-mbar surface). (3rd) Water ice optical depth at 825 cm^{-1}. (Bottom) Water vapor column abundance in precipitable microns (pr-μm). The largest data gaps were caused by solar conjunction and various times when the MGS spacecraft went into contingency (safing) mode.